Journal of Vertebrate Paleontology
Publication details, including instructions for authors and subscription information:
http://www.tandfonline.com/loi/ujvp20

Biological implications of the bone microstructure of the Late Cretaceous Ornithopod Dinosaur Gasparinisaura cincosaltensis

Ignacio A. Cerda [a] & Anusuya Chinsamy [b]

[a] Conicet-Inibioma, museo de Geología y Paleontología, Universidad Nacional del Comahue, Buenos Aires 1400, 8300, Neuquén, Argentina

[b] University of Cape Town, Zoology Department, Private Bag, Rondebosch, 7700, Cape Town, South Africa

Available online: 28 Feb 2012

To cite this article: Ignacio A. Cerda & Anusuya Chinsamy (2012): Biological implications of the bone microstructure of the Late Cretaceous Ornithopod Dinosaur Gasparinisaura cincosaltensis , Journal of Vertebrate Paleontology, 32:2, 355-368

To link to this article: http://dx.doi.org/10.1080/02724634.2012.646804

Journal of Vertebrate Paleontology 32(2):355–368, March 2012

ARTICLE

BIOLOGICAL IMPLICATIONS OF THE BONE MICROSTRUCTURE OF THE LATE CRETACEOUS ORNITHOPOD DINOSAUR *GASPARINISAURA CINCOSALTENSIS*

IGNACIO A. CERDA*[,1] and ANUSUYA CHINSAMY[2]
[1]Conicet-Inibioma, museo de Geología y Paleontología, Universidad Nacional del Comahue, Buenos Aires 1400, 8300 Neuquén, Argentina, nachocerda6@yahoo.com.ar;
[2]University of Cape Town, Zoology Department, Private Bag, Rondebosch 7700 Cape Town, South Africa, Anusuya.Chinsamy-Turan@uct.ac.za

ABSTRACT—Here we present the bone histology of *Gasparinisaura cincosaltensis*, a basal ornithopod from the Late Cretaceous of Patagonia, and discuss its biological implications. The sample includes axial and appendicular elements from several specimens of different ontogenetic stages. The cortex of most bones consists of fibro-lamellar tissue, with mainly longitudinally oriented vascular spaces, which suggests rapid osteogenesis and fast growth. However, the fibro-lamellar bone is commonly interrupted by lines of arrested growth and/or annuli composed of parallel-fibered bone that indicates that the rapid growth was periodic. Although a true outer circumferential layer was not recorded in any of the sampled elements, in several of the larger samples the woven-fibered matrix of the inner and middle cortex grades into a parallel-fibered tissue, which suggests that the attainment of sexual maturity occurred before skeletal maturity. The growth dynamics of *Gasparinisaura* are similar to those reported in other basal ornithopods. Inter-elemental, as well as intraspecific, variations in histology were observed in *Gasparinisaura*. Such variation could be the result of sexual dimorphism, or the effect of localized conditions of growth, or perhaps plasticity in growth in response to local environmental conditions.

INTRODUCTION

Gasparinisaura cincosaltensis is a small-bodied ornithopod dinosaur whose remains have been recovered from Upper Cretaceous strata in Patagonia, Argentina. A large number of specimens have been collected during the last two decades from the locality of Cinco Saltos (Río Negro Province), in mudstones and sandstones of the early Campanian Anacleto Formation, the uppermost portion of the Neuquén Group (Ramos, 1981; Dingus et al., 2000). *G. cincosaltensis* was initially considered to be a basal euiguanodontian (Coria and Salgado, 1996; Salgado et al., 1997; Novas et al., 2004), but more recent cladistic analyses suggest that it is a basal ornithopod (Norman et al., 2004; Cambiaso, 2007). Although the gross skeletal morphology of *G. cincosaltensis* is reasonably well studied (Coria and Salgado, 1996; Salgado et al., 1997; Cambiaso, 2007), little is known about its biology, especially pertaining to its life history strategies and growth patterns.

Bone microstructure provides information about the biology of extinct vertebrates, and has been used extensively for dinosaurs (e.g., Ricqlès, 1980; Chinsamy-Turan, 2005) and non-mammalian therapsids (Botha and Chinsamy, 2000; Ray et al., 2009; Chinsamy-Turan, 2011). Bone microstructure provides a direct record of ontogenetic growth and it gives clues concerning various aspects of dinosaur biology, including growth rates (Ricqlès, 1980; Chinsamy, 1995; Varricchio, 1997; Erickson et al., 2001; Padian et al., 2004; Lehman and Woodward, 2008), longevity (Chinsamy, 1990, 1993; Varricchio, 1993; Sander, 2000; Klein and Sander, 2007; Lee and Werning, 2008), age at maturity (Varricchio, 1993; Sander, 2000; Klein and Sander, 2007; Lee and Werning, 2008), adult size (Sander et al., 2006; Klein and Sander, 2007; Company, 2010; Stein et al., 2010), and ontogenetic stages and timing of sexual maturity (Sander, 2000; Erickson et al., 2007; Lee and Werning, 2008; Klein and Sander, 2008; Hayashi et al., 2009).

Previous work on the bone microstructure of basal ornithopods and basal iguanodontian dinosaurs has contributed significantly to understanding various aspects of their biology (Fig. 1; Winkler, 1994; Chinsamy, 1995; Chinsamy et al., 1998; Horner et al., 2009). Results of these studies indicate that the cortical bone is composed mainly of fibro-lamellar bone tissue, with a lesser amount of parallel-fibered bone tissue. The presence of lines of arrested growth (LAGs) indicates a cyclic growth in some species such as *Orodromeus makelai* (Padian et al., 2004; Horner et al., 2009). However, early studies on the long bone microstructure of some specimens of *Dysalotosaurus* (= *Dryosaurus*) *lettowvorbecki* and *Leallynasaura amicagraphica* did not show any growth marks, which suggested different growth strategies among basal ornithopods and basal iguanodontian dinosaurs (Chinsamy, 1995; Constantine et al., 1998). Recent work on *Dysalotosaurus lettowvorbecki* has found that although rare, a few long bones have localized occurrences of LAGs (which cannot be traced around the compacta), whereas a weak zonation was observed in restricted parts of the compacta, i.e., only along the lateral side of the posterior bone wall (Hübner, 2010). In addition, a more comprehensive study of the Australian polar ornithopods found that the majority of the individuals sampled exhibited LAGs, although only a few showed LAGs associated with annuli (Woodward et al., 2011b). The current study documents the bone histology, inter-elemental histovariability, and ontogenetic changes in the bones of *G. cincosaltensis*. The relative abundance of *G. cincosaltensis* specimens collected to date (Coria and Salgado, 1996; Salgado et al., 1997; Cambiaso 2007; Cerda, 2008) offers an excellent opportunity to study the bone microstructure of this taxon. This work represents the first comprehensive account of the bone microstructure of a South American dinosaur and provides a direct assessment of the growth strategy of *G. cincosaltensis*.

Institutional Abbreviations—**MCS-Pv**, Vertebrate paleontology collection of the Museo Regional Cinco Saltos, Rio Negro Province, Argentina; **MCS-Ph**, Paleohistology collection of the

*Corresponding author.

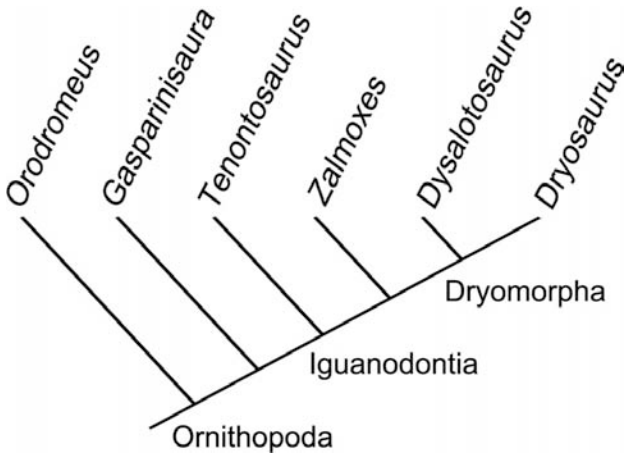

FIGURE 1. Phylogenetic relationships of basal ornithopods and basal iguanodontians for which bone histology has been previously studied. The phylogeny is based on trees given in Norman (2004) and Norman et al. (2004).

Museo Regional Cinco Saltos; **MUC-Pv**, Vertebrate paleontology collection of the Museo de la Universidad Nacional del Comahue, Neuquén Province, Argentina; **NMV**, National Museum of Victoria, Victoria, Australia; **UCT**, University of Cape Town, Cape Town, South Africa.

MATERIALS AND METHODS

Postcranial bones of eleven specimens of *Gasparinisaura cincosaltensis* were used in this study (Table 1). Except for MCS-Pv 109, all specimens have been previously assigned to *G. cincosaltensis* (Salgado et al., 1997; Cambiaso, 2007; Cerda, 2008). The following characters permit referral of MCS-Pv 109 to *G. cincosaltensis*: absence of the anterior intercondylar groove from the femur; lateral condylid of femur laterally placed; and metatarsal II transversely compressed in anterior view (less than 15% of the transverse width of all three metatarsals) (Salgado et al., 1997). All skeletal elements examined were excavated from the outcrops of the Anacleto Formation, near the city of Cinco Saltos.

Because most of the bones obtained for histological sections were fragmentary and the adult size of *G. cincosaltensis* is unknown, the relative size of the specimens was obtained indirectly (see Table 2). For this purpose, detailed anatomical measurements (distance between the anterior trochanter and the lateral condyle of the femur, distance between the lateral condyle and the distal side of the base of the fourth trochanter, metatarsal II length, distance between the anterior trochanter and the femoral head, and distance between the medial and lateral condyles of the femur) of all specimens included in this study, as well as from the holotype (MUC-Pv 208), and also of

TABLE 1. *Gasparinisaura cincosaltensis* specimens and skeletal bones examined for histology.

Specimen number	Slide number	Element(s)	Location and orientation
MCS-Pv 002	MCS-Ph 007	Left tibia and fibula	Proximal metaphysis (T)
	MCS-Ph 008	Left tibia and fibula	Mid-shaft (T)
	MCS-Ph 009	Left tibia and fibula	Proximal end (L)
MCS-Pv 110	MCS-Ph 001	Right femur	Mid-shaft below the fourth trochanter (T)
	MCS-Ph 002	Right femur	Mid-shaft including fourth trochanter (T)
	MCS-Ph 003	Left tibia	Proximal metaphysis (T)
	MCS-Ph 004	Left fibula	Mid-shaft (T)
	MCS-Ph 005	Dorsal rib	Shaft (T)
MCS-Pv 112	MCS-Ph 024	Left scapula	Scapular blade (T)
	MCS-Ph 025	Dorsal rib	Shaft (T)
MUC-Pv 213	MCS-Ph 031	Right femur	Mid-shaft below the fourth trochanter (T)
	MCS-Ph 032	Right femur	Mid-shaft below the fourth trochanter (T)
	MCS-Ph 033	Right femur	Mid-shaft below the fourth trochanter (T)
	MCS-Ph 034	Dorsal rib	Shaft (T)
MUC-Pv 214	MCS-Ph 023	Tibia	Mid-shaft (T)
	UCT 214MTI	Metatarsal	Mid-shaft (L)
MUC-Pv 215	UCT 215FBII	Femur	Distal end (L)
	UCT 215TBII	Tibia	Distal end (T)
	UCT 215vI	Vertebra	Centrum (T)
	UCT 215vII	Vertebra	Centrum (T)
MUC-Pv	UCT 225I	Femur	Distal end (L)
225	UCT 225II	Femur	Proximal end (L)
MCS-Pv 109	MCS-Ph 010	Left tibia	Distal shaft (T)
	MCS-Ph 018	Left tibia and metatarsals II, III, and IV	Mid-shaft (tibia), distal shaft (metatarsals) (T)
	MCS-Ph 019	Left tibia	Proximal metaphysis (T)
	MCS-Ph 022	Metatarsal IV	Mid-shaft (T)
	MCS-Ph 012	Left metatarsal IV	Proximal and mid-shaft (T)
	MCS-Ph 015	Left? metatarsal IV	Distal end (L)
	MCS-Ph 016	Pedal phalanx	Mid-shaft (T)
	MCS-Ph 017	Ungual phalanx	(L)
	MCS-Ph 013	Caudal vertebrae	Centrum (L)
	MCS-Ph 014	Caudal vertebrae	Centrum (L)
	MCS-Ph 020	Caudal vertebra	Centrum (T)
	MCS-Ph 021	Caudal vertebra	Centrum (T)
MCS-Pv 003	MCS-Ph 006	Left femur	Proximal end (L)
MUC-Pv	UCT 227I	Caudal vertebra	Centrum (T)
227	UCT 227II	Caudal vertebra	Centrum (T)
MUC-Pv 218	UCT 218I	Tibia	Distal end (L)

Abbreviations: **L**, longitudinal section; **T**, transverse section.

the most complete individual collected to date (MCS-Pv 111) were taken. The relative size of individuals (represented as percentage of the largest individual [LI]) is expressed in terms of the total length of the femur (femoral length scales isometrically during ontogeny in extant archosaurs; Erickson and Tumanova, 2000). Specimen MUC-Pv 213 is the largest known individual of *G. cincosaltensis* (i.e., 100% of LI). In specimens where no complete femur was available, this measurement was indirectly estimated using the relationship between the total length of the femur and the other bone measurements (e.g., the distance between the lateral condyle and the distal side of the base of the fourth trochanter is around 44% of the total length of the femur). Due to the fragmentary nature of some specimens (e.g., MUC-Pv 218), their relative size could not be estimated.

Specimens were prepared for thin sectioning using the methods outlined in Chinsamy and Raath (1992). The preparation of the histological sections was carried out in Departamento de Geología de la Universidad Nacional de San Luis (Argentina), and at the University of Cape Town in the Department of Zoology, Cape Town. Because this is a destructive method, all specimens were photographed and standard measurements taken before sectioning. The samples were embedded in polyester resin (Emec). All embedded samples were cut using a Buehler Isomet 1000 low speed precision saw with narrow (0.3 mm wide) Diamant Boart diamond blades. After cutting, both sides of the slice were impregnated with a synthetic epoxy resin (Distraltec-ep systems) and mounted on glass. The sections were then ground to the appropriate thinness and polished using a Struers DP-U2 variable speed grinder-polisher with silicon carbide abrasive papers (Buehler Ltd.). The thin sections were studied by light microscopy under normal and polarized light (LabKlass JPL-1350a). Images of each thin section were digitally captured by a digital camera (Canon PowerShot A540). Images of each section were digitally captured with some overlap and were reassembled in Adobe PhotoShop. Histological sections from this study are catalogued into the slide libraries of the MCS and UCT (see access number in Table 1). Nomenclature and definitions of structures used in this study are derived from Francillont-Viellont et al. (1990) and Chinsamy-Turan (2005).

RESULTS

General Histological Features

The transverse sections of all elements show an outer compact cortex surrounding a large medullary region. At the mid-shaft of long bones, there is a free marrow cavity. Cancellous bone infills the medullary regions of ribs, phalanges, caudal vertebrae, and the distal portions of long bones. The predominant tissue in the compacted bone wall is fibro-lamellar bone. The matrix of the cortical bone varies within the cortex in terms of the spatial organization of the collagen fibers. In several samples, the woven-fibered matrix of the inner and middle cortex grades into a parallel-fibered tissue. The channels in the bone (in which vascular canals and other soft tissue are located; Starck and Chinsamy, 2002) are organized as primary osteons, the majority of which are longitudinally oriented. Although not completely accurate, we consider the channels to reflect the extent and organization of 'vascularization.' Compacted coarse cancellous bone tissue is observed at the metaphyseal and epiphyseal regions of the long bones. The cortical bone of some elements (e.g., tibiae, femora) exhibits growth marks that consist of annuli of parallel-fibered bone and/or LAGs. Secondary osteons are observed in the perimedullary region of few samples. Apart these general features, distinctive histological characteristics were observed in the different skeletal elements (see below).

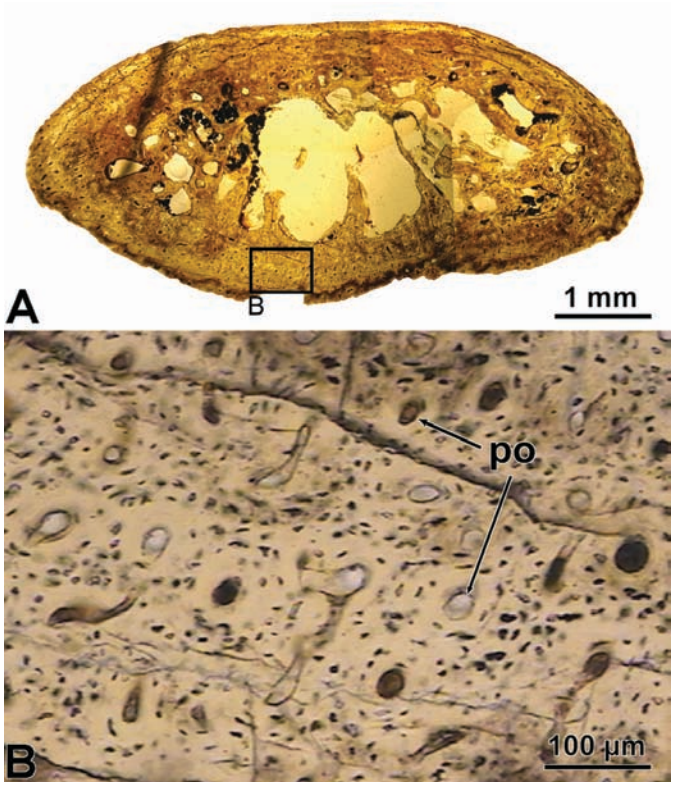

FIGURE 2. Microanatomy and histology of *Gasparinisaura cincosaltensis* scapula (MCS-Pv 112). **A**, general aspect of the mid-shaft cross-section showing the distribution of compact bone and medullary spaces; **B**, detail of the fibro-lamellar bone tissue. Note the abundance of longitudinally oriented primary osteons. Normal light. **Abbreviation**: **po**, primary osteons. (Color figure available online.)

Scapula

A single thin section of a scapula was obtained from one of the smallest individuals (MCS-Pv 112; 56% of LI). In cross-section, the anterior portion of the scapular blade reveals a wide marrow cavity with reconstructed endosteal bony trabeculae (Fig. 2A). Medullary cancellous spaces are surrounded by lamellar bone. The cortex consists of uninterrupted fibro-lamellar bone tissue. The woven bone matrix contains abundant globular osteocyte lacunae that are randomly arranged. The cortical tissue is well vascularized, with many longitudinal and some radial canals (Fig. 2B). In the lateral part of the cortex, the density of primary osteons and osteocyte lacunae tends to diminish. No growth marks are evident.

Femur

Cross-sections of the femora of two individuals (MCS-Pv 110 and MUC-Pv 213; 86% and 100% of LI, respectively) were studied. The femoral shaft in both specimens shows a cortical region composed of compact bone and a large marrow cavity (Fig. 3A, B).

In the mid-shaft region of MCS-Pv 110, a thin layer of circumferential endosteal lamellar tissue, containing flattened osteocyte lacunae, surrounds the medullary cavity (the inner circumferential layer, ICL). Some radial 'vascular' canals connect the marrow cavity with the cortex. The cortical bone consists of primary bone organized in alternating zones and annuli (Fig. 3C–E). The zones comprise highly vascularized fibro-lamellar bone tissue, which is isotropic under polarized light (except on its primary osteons,

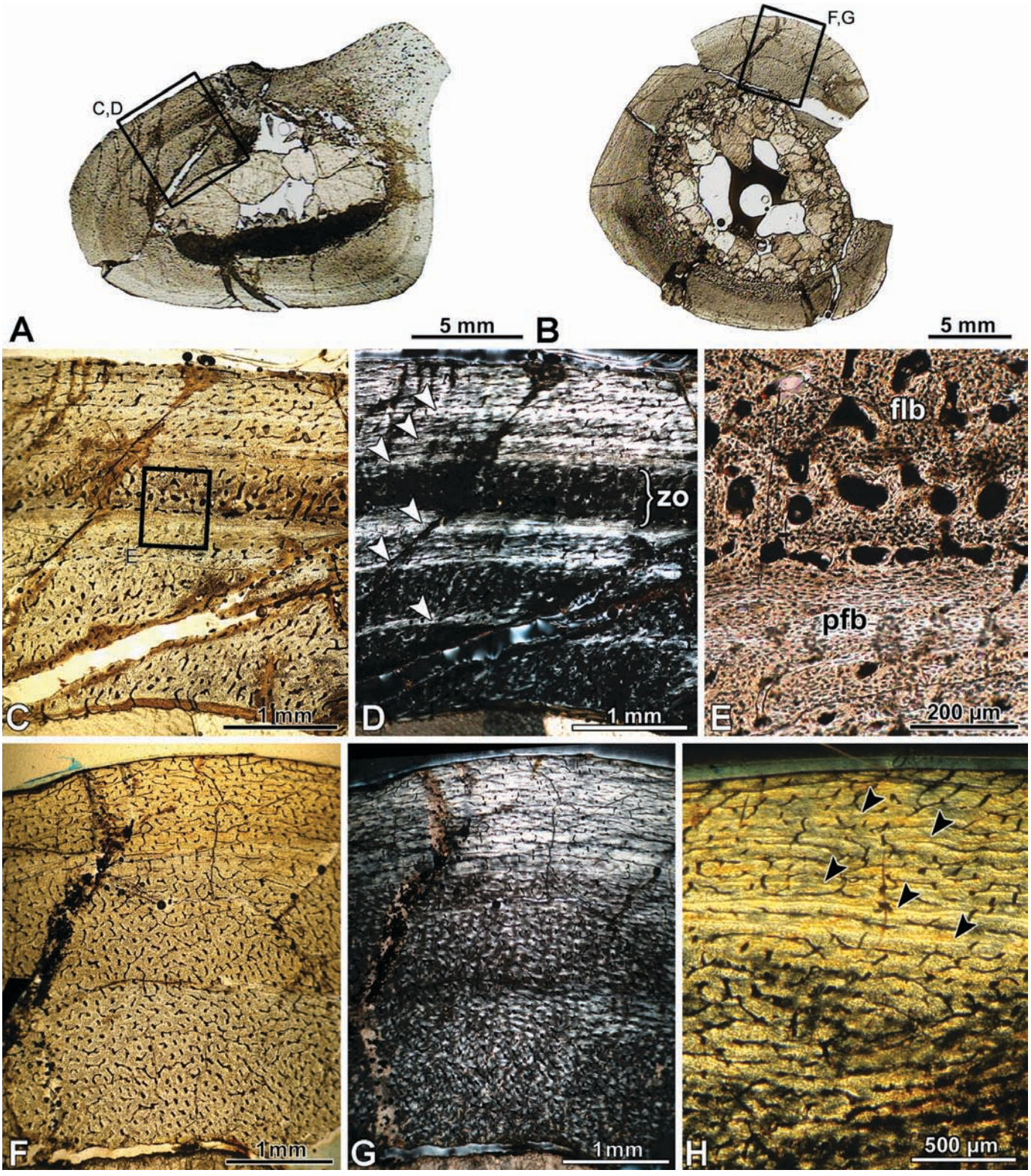

FIGURE 3. Microanatomy and histology of *Gasparinisaura cincosaltensis* femora. **A**, **B**, general aspect of the mid-shaft cross-section of MCS-Pv 110 (**A**) and MUC-Pv 213 (**B**). The slice in **A** includes part of the fourth trochanter; **C**, **D**, cortical bone tissue viewed under normal (**C**) and polarized (**D**) light showing alternating zones and annuli (arrowheads). Note the high birefringence of the annuli and the isotropic nature of the zones under crossed nicols; **E**, transition between an annulus of parallel-fibered bone and a zone of fibro-lamellar bone; **F**, **G**, cortical bone tissue viewed under normal (**F**) and polarized (**G**) light. Whereas the inner and middle cortex is isotropic, the external cortex is anisotropic; **H**, LAGs (arrowheads) in the external cortex of the same specimen. Note that whereas the growth marks in MCS-Pv 110 are distributed in the whole cortex, such marks are restricted to the external cortex in MUC-Pv 213. **Abbreviations**: **flb**, fibro-lamellar bone; **pfb**, parallel-fibered bone; **zo**, zone.

which are composed of anisotropic lamellar tissue). Osteocyte lacunae are globular and randomly distributed in the woven matrix. In the innermost region, the zones are thick, the 'vascular' canals are wide and they are longitudinally and obliquely arranged. In the outer cortex, the zones tend to be narrow, the organization of the 'vascular' channels is laminar, and the size of the lumen is small. Also, the woven component of the fibro-lamellar tissue becomes more organized and slightly anisotropic under polarized light. The annuli consist of poorly 'vascularized,' parallel-fibered bone tissue with flattened osteocyte lacunae that are arranged in parallel. The fibrillar organization of the outer cortex changes to a parallel-fibered bone tissue, making it more difficult to accurately discern the number of growth rings. However, because under polarized light the annuli are more birefringent, six annuli were observed (Fig. 3D). Additionally, at least two lines of arrested growth (LAGs) are observed in the cortex. One of the thin sections (MCS-Ph 002) includes part of the fourth trochanter, which consists of a large amount of compacted coarse cancellous bone in the inner cortex. The external cortex of the fourth trochanter is rich in Sharpey's fibers and the channels in the bone have a radial orientation.

The transverse sections obtained from the largest individual (MUC-Pv 213) also exhibit a large medullary cavity surrounded by a thin layer of endosteal lamellar tissue. The cortex is composed of highly vascularized fibro-lamellar bone tissue (Fig. 3F). In the perimedullary region, woven-fibered bone matrix consists of loosely packed collagen fibers distributed without any spatial organization. Osteocyte lacunae are globular and randomly oriented in this region. This pattern changes toward the external cortex, where the woven-fibered matrix of the fibro-lamellar bone grades into a more spatially organized (parallel-fibered) bone tissue (Fig. 3G). The osteocyte lacunae tend to be flattened and spatially organized at the periphery of the cortex. The outer compacta is interrupted by five closely spaced LAGs, which are sometimes associated with annuli (Fig. 3H). The annuli consist of less vascularized, parallel-fibered bone tissue containing flattened osteocyte lacunae, which are spatially organized. The entire cortex is highly 'vascularized,' but the 'vascular' pattern is variable in different regions of the same section. The inner cortex contains abundant primary osteons with wide canals arranged in an irregular pattern. This pattern is most pronounced in the anterolateral portion. The outer cortex exhibits primary osteons with small vascular spaces longitudinally and circumferentially arranged, with oblique anastomoses. Although in regions near the sub-periosteal margin the bone is poorly vascularized, the bone tissue is never avascular and in several instances numerous canals open to the sub-periosteal surface. A small region of compacted coarse cancellous bone is observed at the lateral side of the perimedullary cortex. Few secondary osteons are recognized in this region.

Longitudinal sections of the femora of three individuals (MUC-Pv 225, MCS-Pv 003, and MUC-Pv 215; 49%, 79%, and 82% of LI, respectively) were made (Fig. 4). The proximal section of MCS-Pv 003 reveals the internal microanatomy of the femoral head and also demonstrates that the greater trochanter is composed of fine cancellous bone tissue. The cancellous spaces in the metaphyseal region are more enlarged than those observed in the 'epiphysis.' The thickness of the compact bone in the metaphyseal region decreases toward the epiphyseal end. In the smaller individual, the calcified cartilage is extensively developed; islands of calcified cartilage are evident in several of the bony struts, and the calcified cartilage extends to the end of the bone. In the larger femora sampled, the amount of calcified cartilage is reduced, but even in the largest femur some calcified cartilage is present.

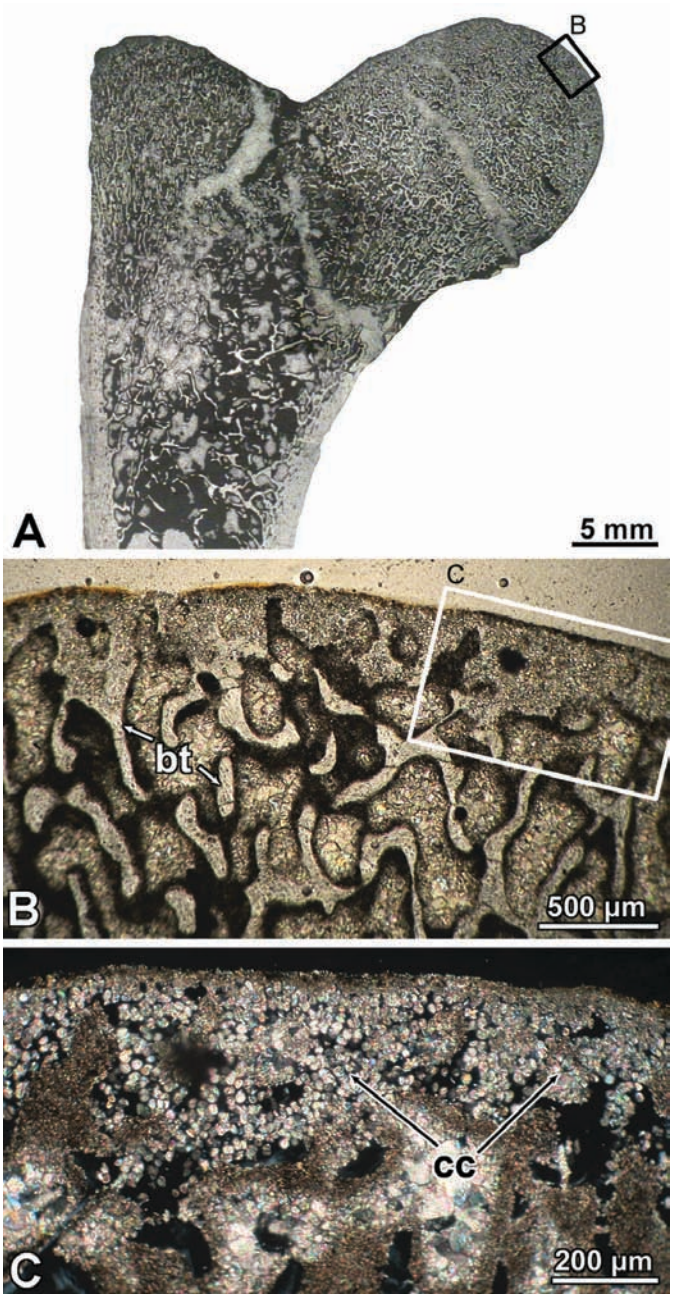

FIGURE 4. Microanatomy and histology of *Gasparinisaura cincosaltensis* femur (MCS-Pv 003). **A**, general view of the longitudinal section of the proximal end. The element is mainly composed of cancellous bone tissue; **B**, detail of the 'articular' surface showing a thin layer of calcified cartilage. Groups of calcified cartilage lacunae are visible in some bony trabeculae; **C**, detail of the calcified cartilage. Note the globular shape of the cartilage lacunae. **Abbreviations**: **bt**, bony trabeculae; **cc**, calcified cartilage. (Color figure available online.)

Tibia

Several sections in the diaphyseal and metaphyseal regions of six tibiae were examined (Table 2). In all of the sampled elements, the mid-shaft sections reveal a medullary cavity surrounded by a thick wall of compact bone (Fig. 5A–C).

In the section obtained from the mid-shaft of the smallest specimen (MCS-Pv 002; 48% of LI), the cortex comprises fibro-lamellar tissue with predominantly longitudinally oriented primary osteons, although some radial and oblique canals are also observed, and 'vascularization' tends to decrease toward the peripheral margin of the bone wall. The woven matrix contains several globular osteocyte lacunae that are haphaz-

TABLE 2. Bone measurements and relative size of *Gasparinisaura cincosaltensis*.

Specimen	T-wp	MII-l	F-wd	F-wp	F-pf	F-l	PLI
MUC-Pv 208*	25.3	51	19.5	20.7	39.7	88.2	55%
MCS-Pv 111*	—	67	—	—	49	114.7	71%
MCS-Pv 002	22	—	—	—	—	77**	48%
MCS-Pv 003	—	—	—	30.2	—	127**	79%
MCS-Pv 110	39.7	80	—	—	—	138**	86%
MCS-Pv 112	—	—	18.5	—	—	89	56%
MUC-Pv 213	—	—	—	36.5	70	160**	100%
MUC-Pv 215	—	—	29.3	—	—	132**	82%
MUC-Pv 225	—	—	17.4	17.8	—	78**	49%
MCS-Pv 109	—	—	27.9	—	—	130**	81%

Measurements where obtained from the most complete specimens of *G. cincosaltensis* (MUC-Pv 208, MUC-Pv 213, and MCS-Pv 111) and the specimens sectioned for this study. All measurements in mm. **Abbreviations**: **F-l**, distance between the anterior trochanter and the lateral condyle of the femur; **F-pf**, distance between the lateral condyle and the distal side of the base of the fourth trochanter; **F-wd**, distance between the lateral and medial condyles of the femur; **F-wp**, distance between the anterior trochanter and the femoral head; **MII-l**, metatarsal II length; **T-wp**, anteroposterior width of the proximal end of the tibia; **PLI**, percentage of largest individual.
*Specimens not included in the histological sample.
**Values only approximated because they were obtained indirectly.

ardly distributed. Two ill-defined annuli are visible: one in the middle cortex, and the other in the external-most part of the cortex (Fig. 5D). Each 'annulus' is characterized by a relatively low density of flattened osteocyte lacunae. Also, the fiber arrangement of the woven matrix has a slightly more ordered arrangement, being rather anisotropic under polarized light. An isolated, conspicuous open space is visible in the cortex on the medial region. Few layers of lamellar bone tissue surround this cavity. An inner circumferential layer (ICL) is absent around the medullary cavity. In the metaphyseal region, a narrow region of cortical bone consisting mainly of compacted coarse cancellous tissue occurs. The outermost portion of the cortex exhibits a layer of fibro-lamellar bone tissue, which is poorly vascularized near the sub-periosteal margin. Trabeculae of cancellous bone are visible in the medullary cavity.

In one of the medium-sized specimens (MCS-Pv 109; 81% LI), sections of the tibia in the mid-shaft, distal shaft, and proximal metaphysis were obtained. In sections from the mid-shaft region, a distinct ICL occurs around the medullary cavity and consists of endosteally formed lamellar tissue (Fig. 5E). This layer is less developed in the distal shaft and metaphyseal regions, where cancellous spaces and bony trabeculae become more extensively developed near the medullary cavity. Extensive compacted coarse cancellous bone is seen in the perimedullary region, and is often distinctly separated from periosteal growth by a distinct reversal line (Fig. 5F). The thickness of this endosteal tissue varies in the different portions of the element, being more developed in the metaphyseal region. The middle and external cortex consists of fibro-lamellar tissue (Fig. 5G). The bone matrix of the fibro-lamellar tissue is not quite irregularly woven as one would expect; polarized light reveals that most fibers are well organized (general anisotropy under crossed nicols). Also, the osteocyte lacunae tend to be spindle-shaped. This kind of fibro-lamellar bone tissue (highly vascularized but with no true woven component) has been recognized previously in pseudosuchian archosaurs and other non-avian dinosaurs (Ricqlès et al., 2003, 2008; Stein et al., 2010). The arrangement of the 'vascular' canals is mainly circumferential in the mid-shaft and longitudinally in the distal shaft. In the metaphyseal section, the layer of fibro-lamellar bone is poorly developed or absent, and the compacted coarse cancellous bone is followed by a layer of parallel-fibered bone. Regarding the presence of growth marks, fibro-lamellar tissue is interrupted by LAGs and annuli of parallel-fibered bone. The number of growth marks varies in the element (two LAGs and annuli in the mid-shaft, one LAG and an annulus in the distal shaft). In the distal shaft, some secondary osteons are evident in the perimedullary region. As in the smaller specimen (MCS-Pv 002), an open space, surrounded by lamellar bone, is visible in the fibro-lamellar cortex at the mid-shaft. Evidence of bone remodeling (i.e., the process of resizing and reshaping of the tibia during development) is more clearly visible in the distal shaft regions of the bones.

In MCS-Pv 110 (86% of LI), the microstructure of the bone at the proximal metaphysis is similar to that described for MCS-Pv 109. The cortical bone shows a relatively large medullary cavity, surrounded by a thick layer of circumferentially formed endosteal lamellar bone (Fig. 5H). The inner region of the compact bone wall consists of compacted coarse cancellous bone tissue separated from periosteal growth by a distinct reversal line (Fig. 5I). The middle and outermost region is composed by fibro-lamellar bone tissue where the intrinsic fibers are rather spatially ordered. Only two LAGs are observed in the cortical bone.

A sample obtained from a sub-adult specimen (MCS-Pv 214), probably between 50% and 70% of LI, exhibits richly vascularized fibro-lamellar tissue in the distal shaft. The woven matrix of the fibro-lamellar bone is slightly more organized in the external regions of the compacta. The overall 'vascular' organization is plexiform in the innermost region and laminar in the outermost region. The density of primary osteons decreases towards the periphery. In some areas (posteromedial cortex), the 'vascular' organization is strongly radial. Two annuli are evident in cortical bone.

Longitudinal sections were made from three specimens (MCS-Pv 002, MUC-Pv 215, and MUC-Pv 218). The microanatomy of the proximal and distal ends of the tibiae is composed of fine cancellous bone. In all the samples, 'articular' ends contain a narrow layer of well-preserved calcified cartilage. This layer contains ovoid chondrocyte cell lacunae, which have an irregular arrangement. The cancellous bone is composed of trabeculae of endosteal lamellar bone, which contains elongated cell lacunae. Small islands of calcified cartilage can sometimes be observed within the bony trabeculae.

Fibula

Thin sections from small (MCS-Pv 002; 48% of LI) and medium-sized (MCS-Pv 110; 86% of LI) specimens where obtained. Fibula samples of MCS-Pv 002 include sections from the mid-shaft and proximal metaphyseal region. The only section from MCS-Pv 110 was obtained from the mid-shaft region. In both specimens, fibulae are kidney-shaped in cross-sections of the mid-shaft region and reveal a distinct marrow cavity surrounded by endosteal lamellar bone tissue (Fig. 6A, B). The ICL is

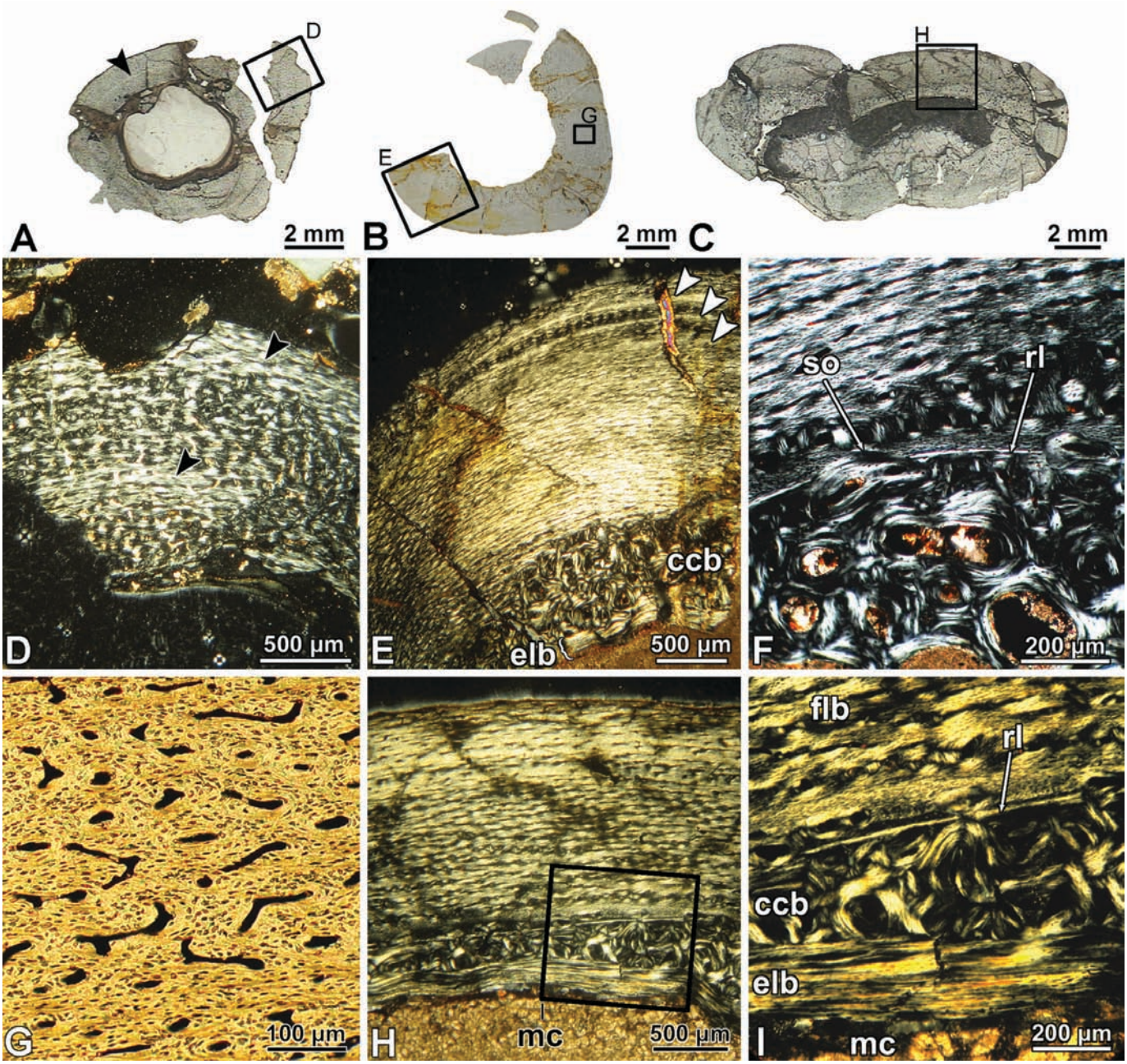

FIGURE 5. Microanatomy and histology of *Gasparinisaura cincosaltensis* tibiae. **A**–**D**, general view of mid-shaft (**A**, **B**) and proximal metaphyseal (**C**) cross-sections of MCS-Pv 002 (**A**), MCS-Pv 109 (**B**), and MCS-Pv 110 (**C**). The arrowhead in **A** indicates an ill-defined annulus; **D**, diaphyseal cross-section showing two ill-defined annuli (arrowheads). The view in polarized light elucidated the more ordered arrangement of the collagen fibers in these structures; **E**, cortical bone tissue viewed under polarized light. The outer cortex reveals three well-defined LAGs and annuli (arrowheads). The inner cortex shows an ICL of lamellar bone tissue. Note the abrupt change between the compacted coarse cancellous bone and the periosteal tissue in the inner cortex; **F**, diaphyseal cross-section of the distal shaft of the same specimen under polarized light (inner cortex). A secondary osteon interrupts the reversal line; **G**, close up of the well-vascularized fibro-lamellar bone tissue at the middle cortex; **H**, cross-section of the proximal metaphyseal region under polarized light. The medullary cavity lacks any bony trabeculae; **I**, detail of the inner cortex of the same specimen showing compacted coarse cancellous bone packed between a thick layer of endosteal lamellar bone and fibro-lamellar bone. Note that whereas the perimedular area of the smaller specimen (MCS-Pv 002) is composed entirely of fibro-lamellar bone tissue, this region contains an OCL of lamellar bone tissue in the other specimens. **Abbreviations**: **ccb**, compacted coarse cancellous bone; **elb**, endosteal lamellar bone; **flb**, fibro-lamellar bone; **mc**, medullary cavity; **rl**, reversal line; **so**, secondary osteon.

vascularized by some radial vascular canals. The cortex at the diaphyseal section is composed of fibro-lamellar bone tissue with longitudinally oriented primary osteons. Vascularization and osteocyte lacunae density are reduced towards the external margin. Growth marks are present in the cortex of both specimens, in which the fibro-lamellar compacta is interrupted by distinct annuli of parallel-fibered bone tissue.

Histological differences are observed among the fibulae sampled. An isolated secondary osteon is visible at the lateral side of the inner cortex from the mid-shaft of MCS-Pv 002. The

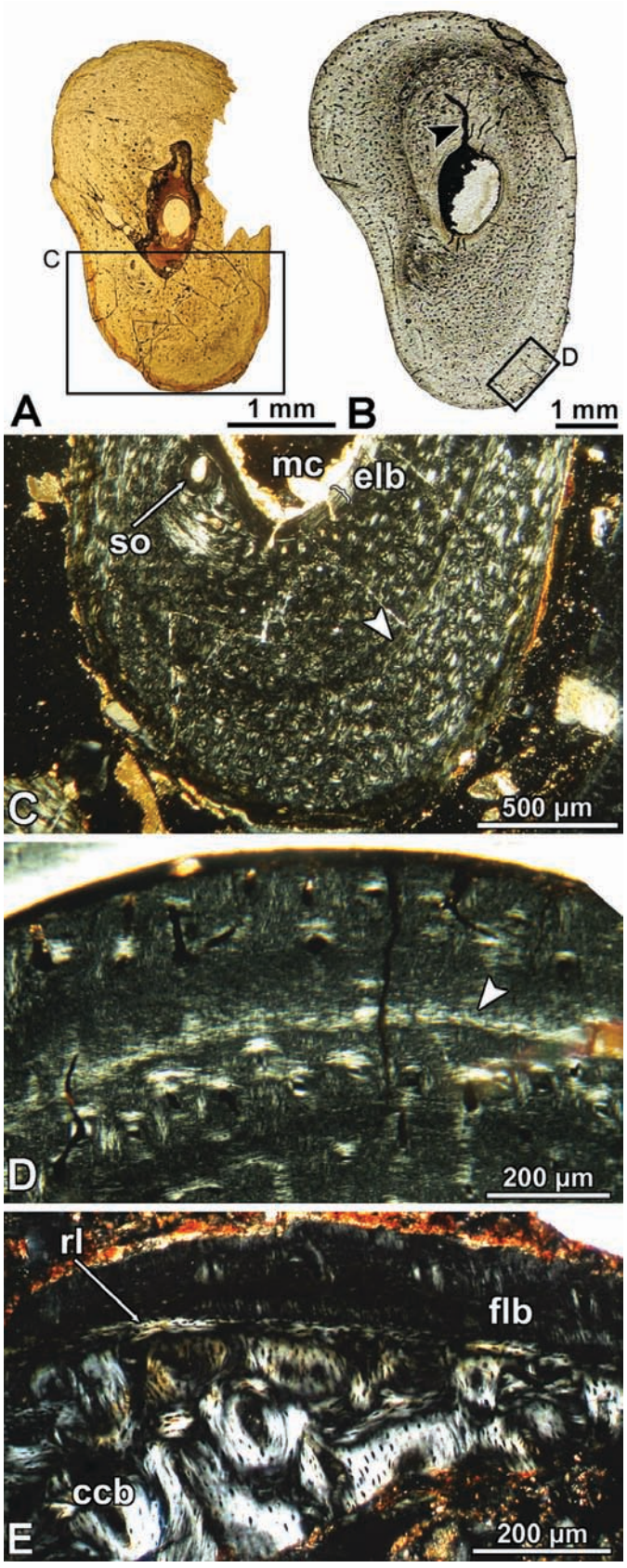

mid-shaft section of MCS-Pv 110 shows a distinctive channel (with multiple subdivisions) that extends from the medullary cavity to the mid-cortical region (Fig. 6B). Also, bone drift is evident in the perimedullary regions of this section. In specimen MCS-Pv 002, an isolated, ill-defined annulus is visible in the compacta (Fig. 6C). LAGs are absent in this sample. By contrast, in MCS-Pv 110, at least two LAGs and one annulus of parallel-fibered bone are present in the external cortex (Fig. 6D).

The deep cortex of the proximally located specimen MCS-Pv 002 is predominantly composed of compacted coarse cancellous bone tissue. The outermost region consists of a narrow band of poorly vascularized fibro-lamellar bone tissue, separated from the endosteal tissue by a reversal line (Fig. 6E).

Metatarsals

Metatarsal thin sections were obtained from MCS-Pv 109 (81% of LI) and MUC-Pv 214 (undetermined PLI). Metatarsals are characterized by the presence of a medullary cavity surrounded by a layer of endosteal lamellar bone tissue in the mid-shaft. This layer disappears towards the ends of the bones, where cancellous spaces and bony trabeculae near the medullary cavity become more extensive (Fig. 7A–C). In cortical bone, the perimedullary region consists of well-vascularized fibro-lamellar bone tissue with haphazardly arranged, globular osteocyte lacunae (Fig. 7D). In the external-most part of the cortex, the woven component of the matrix is more spatially organized, containing mostly flattened, spatially well-organized osteocyte lacunae. Compacted coarse cancellous bone tissue is observed in the innermost regions in sections sampled from the end of the bones (metaphyseal region). Layers of poorly vascularized, parallel-fibered bone tissue are present in the outermost region of some sections (MCS-Ph 012, MCS-Ph 022), particularly in the articulation contact regions (e.g., in metatarsal IV, the surface of contact with metatarsal III). In a section obtained from the shaft of the metatarsal IV (MCS-Ph 012), the transition from endosteal lamellar, compacted coarse cancellous, fibro-lamellar, and parallel-fibered bone is clearly evident (Fig. 7E–F). A distinct reversal line demarcates the endosteal and periosteal bone tissues. 'Vascular' orientation varies between different bones, different areas of the same bone, and different areas of the same thin section. A single LAG is observed in the external region of metatarsal IV (MCS-Ph 018, MCS-Ph 012). Secondary osteons were only present in a single thin section from metatarsal IV (MCS-Ph 022). In this section, secondary osteons occupy the perimedullary region, reaching the middle and the outer cortex in some places.

A longitudinal section from the distal end of a metatarsal IV was studied. As described in the other longitudinal sections, the distal end is almost entirely composed of fine cancellous bone, produced by endochondral replacement of calcified cartilage near the 'articular' surface. The cancellous spaces of the

← FIGURE 6. Microanatomy and histology of *Gasparinisaura cincosaltensis* fibulae. **A**, **B**, general aspect of the mid-shaft cross-section of MCS-Pv 002 (**A**) and MCS-Pv 110 (**B**). Note a distinctive channel (with multiple subdivisions) that extends from the medullary cavity to the mid-cortical region in specimen MCS-Pv 110 (arrowhead); **C**, viewed under polarized light showing an ill-defined annulus (arrowhead). Note the presence of an inner circumferential layer of lamellar bone tissue surrounding the medullary cavity; **D**, annulus of parallel-fibered bone tissue in the outer cortex (arrowhead); **E**, detail of the cortical tissue in the proximal metaphyseal region of MCS-Pv 002. The coarse compacted bone tissue is separated from the fibro-lamellar bone by a reversal line. **Abbreviations**: **ccb**, coarse compacted bone tissue; **elb**, endosteal lamellar bone; **flb**, fibro-lamellar bone; **mc**, medullary cavity; **rl**, reversal line; **so**, secondary osteon. (Color figure available online.)

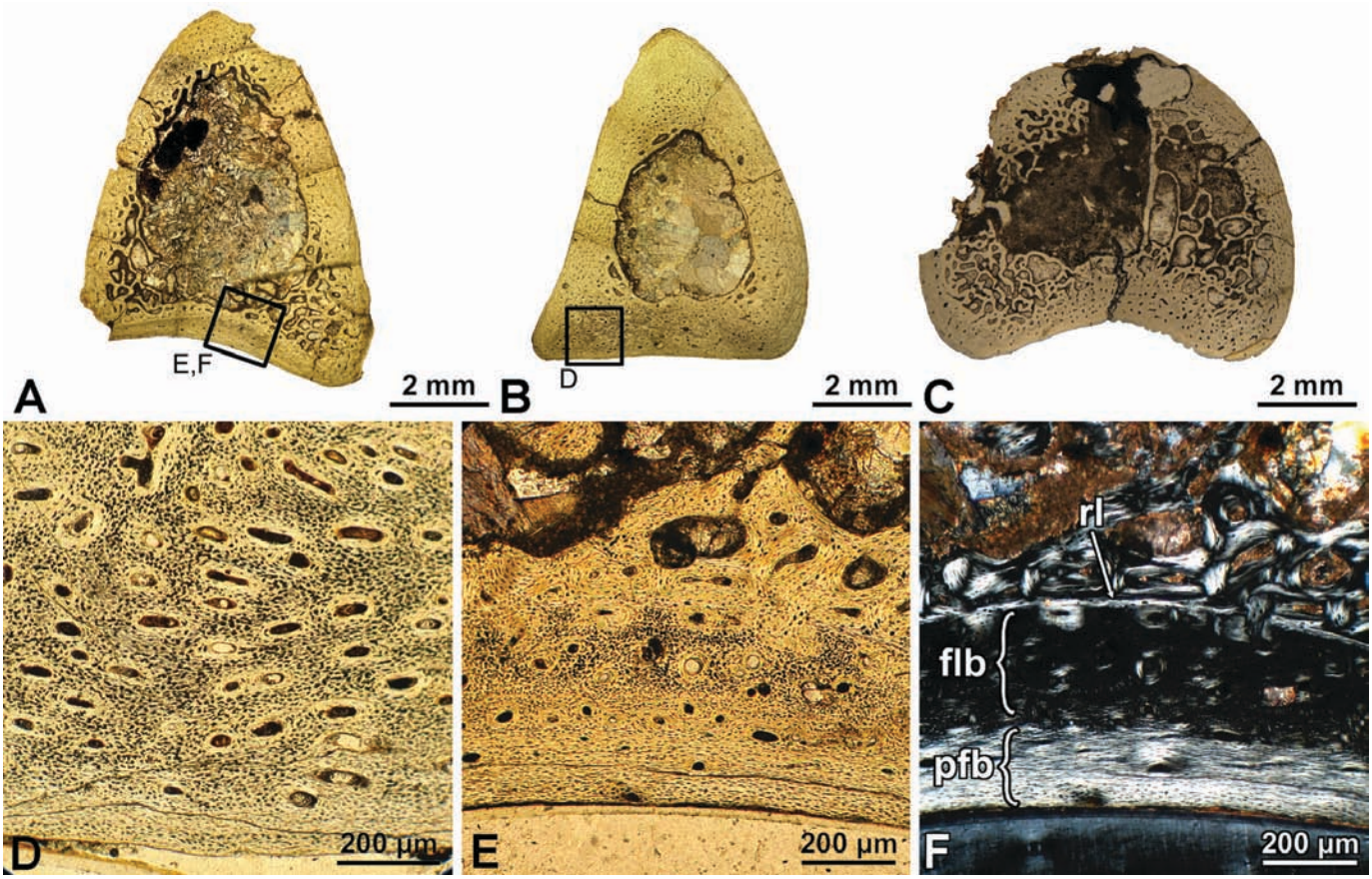

FIGURE 7. Microanatomy and histology of *Gasparinisaura cincosaltensis* metatarsal IV (specimen MCS-Pv 109). **A**–**C**, general aspects of the proximal (**A**), mid- (**B**), and distal shaft (**C**) cross-sections. Note the higher abundance of cancellous bone toward the epiphyseal regions; **D**, detail of the well-vascularized fibro-lamellar bone tissue in the outer cortex; **E**–**F**, enlarged view of the cortical bone under normal (**E**) and polarized (**F**) light. Note the rather abrupt transition between the inner, isotropic, fibro-lamellar bone and the outer, anisotropic, parallel-fibered bone tissue. This transition contrasts with the homogeneous development of fibro-lamellar bone tissue in the mid-shaft of the same specimen (**D**). **Abbreviations**: **flb**, fibro-lamellar bone; **pfb,** parallel-fibered bone tissue; **rl**, resorption line.

spongy bone in the metaphyseal region are more enlarged. A thin coating of calcified cartilage is clearly observed in most of the 'articular' surface and some groups of cartilage lacunae are also visible within the bony trabeculae of the more distal cancellous bone.

Pedal Phalanx

The transverse section of a proximal phalanx (MCS-Pv 109) shows a narrow cortex composed of fibro-lamellar bone (Fig. 8A). Most of the vascular canals are longitudinally oriented. In the outer region, the cortical bone is less vascularized and fibers of the woven matrix are more spatially organized. Also, osteocyte lacunae are flattened and circumferentially organized. Sharpey's fibers are evident in the fibro-lamellar tissue, and are obliquely oriented with respect to the external margin (Fig. 8B). The medullary region is completely filled with a dense network of bony trabeculae. Some secondary osteons occur in the perimedullary region.

Ungual Phalanx

A horizontal section obtained from MCS-Pv 109 (Fig. 9A) is composed mostly of compact fibro-lamellar bone tissue. The primary osteons have a predominantly longitudinal arrangement with lateral branching canals (Fig. 9B). 'Vascular' spaces are wider toward the distal end. Few secondary osteons are present in the cortex. The lateral grooves of the ungual phalanx are composed of poorly vascularized, parallel-fibered bone tissue that contains two LAGs in the outermost cortex. Sharpey's fibers are abundant in this region (Fig. 9C). The proximal end shows a small, sub-triangular medullary area completely filled with bony trabeculae of cancellous bone. The 'articular' surface is formed by a thin coating of hypertrophied calcified cartilage (Fig. 9D). In this layer, the globular cartilage cell spaces are organized mostly in vertical rows.

Dorsal Ribs

The transverse sections obtained from MCS-Pv 112, MCS-Pv 110, and MUC-Pv 213 have a distinct outer cortex surrounding a medullary region (Fig. 10A–C). MCS-Pv 112 and MCS-Pv 110 rib samples have an elliptical shape, but MUC-Pv 213 is flattened lateromedially. Although all sections exhibit an internal medullary region of cancellous bone, in MUC-Pv 213 this is extensively developed and extends over almost the entire area of the ribs (reaching the outermost region in some areas). In MUC-Pv 213, the cortex is narrow and poorly vascularized in comparison with the other samples.

In all of the samples analyzed, the compact cortex is composed of primary fibro-lamellar bone tissue (Fig. 10D). Vascular spaces

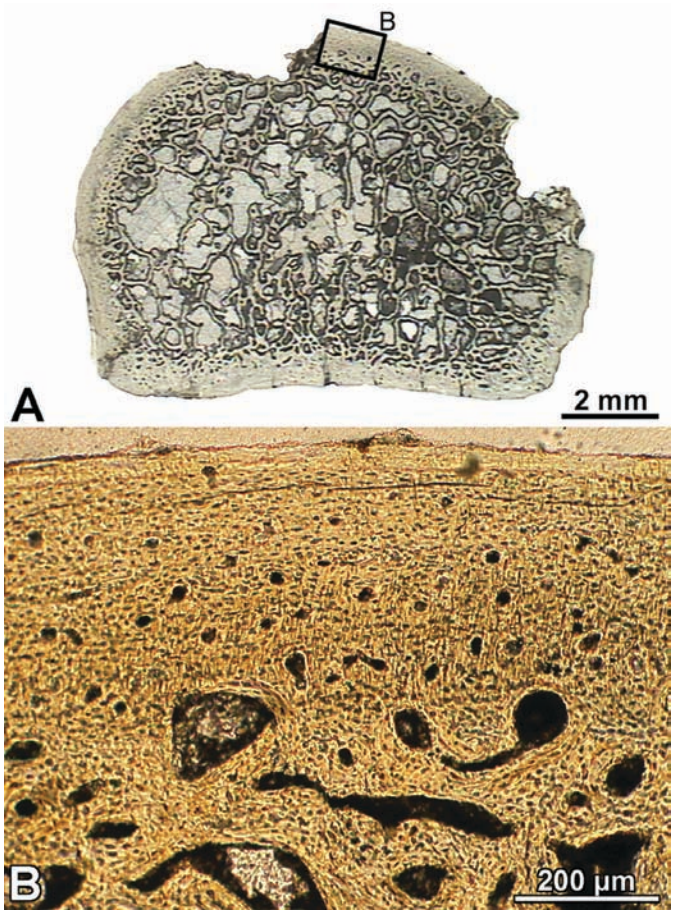

FIGURE 8. Microanatomy and histology of *Gasparinisaura cincosaltensis* pedal phalanx (MCS-Pv 109). **A**, general view of the transverse section. The element is composed of a thin cortex of compact bone surrounding a large medullary region of cancellous bone; **B**, detail of the cortical tissue. Abundant Sharpey's fibers are located in the fibro-lamellar bone. (Color figure available online.)

are mainly longitudinally oriented. Medullary cancellous spaces are surrounded by endosteal lamellar bone (Fig. 10E). An isolated annulus of parallel-fibered bone is evident in the cortex of MCS-Pv 110 (Fig. 10F). In the same specimen, a thin birefringent line is observed in cortical tissue. No LAGs or annuli were observed in the cortical bone at MCS-Pv 112 and MUC-Pv 213.

Caudal Vertebrae

Transverse and longitudinal sections were obtained from the middle caudal vertebrae of MCS-Pv 109 and MUC-Pv 227. The transverse sections exhibit a hexagonal shape and are characterized by a prominent medullary cavity surrounded by a narrow cortex (Fig. 11A). The medullary cavity is occupied by a dense network of cancellous bone trabeculae. The transition between cancellous and cortical bone is rather abrupt and is demarcated by a thin reversal line (Fig. 11B). The fibro-lamellar cortical bone tissue is well vascularized, containing mainly longitudinally oriented primary osteons (few radial canals are also observed). Numerous Sharpey's fibers, obliquely orientated to the external surface, are imbibed in the compacta (Fig. 11C). Longitudinal sections include fragments of two articulated centra. The 'articular' surfaces of the centra are coated by a layer of calcified cartilage. Cancellous bone contacts the layer of calcified cartilage and many chondrocyte lacunae are present inside the trabeculae of endosteal bone.

DISCUSSION

Growth Pattern

The overall distinctive feature throughout ontogeny of the compact cortex of both appendicular and axial bones of *Gasparinisaura cincosaltensis* is the predominance of fibro-lamellar bone tissue. Fibro-lamellar bone is generally considered to be the result of relatively rapid rates of bone deposition (Francillon-Vieillot et al., 1990; Reid, 1996; Chinsamy-Turan, 2005) and therefore suggests an overall fast rate of growth for *Gasparinisaura*. In the smaller specimens (48% and 56% of LI), the fibro-lamellar tissue is continuously deposited or interrupted by poorly defined annuli. In specimens of size of more than 80% of LI, the periosteal bone is interrupted by well-defined annuli with associated LAGs. Also, the 'woven' component of the fibro-lamellar tissue is more spatially organized. Thus, the bone histology of *G. cincosaltensis* suggests high, sustained rates of growth during the early stages of ontogeny, with some indications of a slight decrease in bone deposition (indicated by the presence of poorly developed annuli). During later stages of ontogeny, LAGs and well-defined annuli occur, revealing periodic slow down and/or complete cessation of growth. The annuli and LAGs were commonly followed by a resumption of rapid growth, as shown by the presence of wide zones of fibro-lamellar bone. An overall decrease in the bone depositional rates is indicated in the femora by a change from a woven to a more spatially organized fibrillar matrix of the periosteal bone tissue. As has been proposed in other dinosaurs (Sander, 2000; Erickson et al., 2007) and pterosaurs (Chinsamy et al., 2009), this change from fibro-lamellar bone to parallel-fibered bone probably marks the onset of sexual maturity in *G. cincosaltensis*.

The growth strategy of *G. cincosaltensis* is comparable with that reported for some basal ornithopods and basal iguanodontian dinosaurs, but differs from that of others. For example, the bone histology of *Orodromeus makelai* indicates that this small ornithopod dinosaur grew at rapid rates, but with cyclic (annual) interruptions during development (Padian et al., 2004; Horner et al., 2009). The variable occurrence of LAGs and inconsistent, rather diffuse, faint zonation in *Dysalotosaurus lettorwvorbecki* directly indicates strong individual variability within single individuals and within a single population (Hübner, 2010). The histological features recorded among basal ornithopods and basal iguanodontians generally suggests a cyclical growth pattern reflected by the presence of alternating zones and annuli (and/or LAGs), like those described for *G. cincosaltensis*, although it appears that there is a large amount of variability in terms of presence or absence of growth marks, even within the same individual, and within single bones (e.g., Chinsamy, 1995; Hübner, 2010; Woodward et al., 2011b).

Determinate Growth and Adult Size

The outer circumferential layer (OCL; also referred to as the external fundamental system or EFS) is an informative feature in paleohistological studies because it signals skeletal maturation and slowing down in the rate of bone deposition (Chinsamy-Turan, 2005; Woodward et al., 2011a). This histological feature is typical of animals with determinate growth and consists of either lamellar or parallel-fibered bone, is completely avascular, and may or may not have annuli or LAGs (Chinsamy-Turan, 2005). In our sample, although the arrangement of the intrinsic fibers in the outer cortex of some specimens becomes parallel, the bone tissue is never avascular. The absence of a true OCL in all the studied specimens of *Gasparinisaura cincosaltensis* may be explained by two hypotheses: (1) the growth of *G. cincosaltensis*

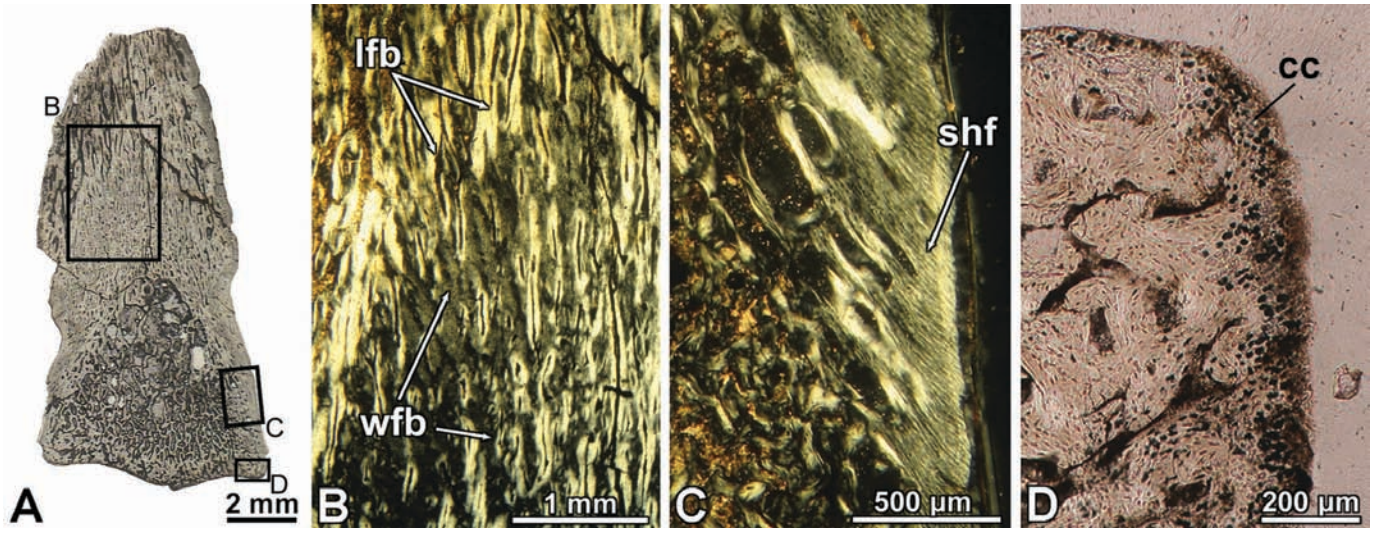

FIGURE 9. Microanatomy and histology of *Gasparinisaura cincosaltensis* ungual phalanx (MCS-Pv 109). **A**, general view of the complete longitudinal section. Note the prevalence of cancellous bone near the articular surface; **B**, close up of the fibro-lamellar bone tissue. The optical properties of the lamellar fibered bone tissue of the primary osteons allows its differentiation from the woven-fibered bone of the matrix; **C**, abundant Sharpey's fibers in the outer lateral cortex; **D**, close up of the articular surface showing a thin layer of calcified cartilage. **Abbreviations**: **cc**, calcified cartilage; **lfb**, lamellar fibered bone; **shf**, Sharpey's fibers, **wfb**, woven-fibered bone. (Color figure available online.)

was indeterminate, or (2) no fully grown specimens are present in our sample. Given that a well-developed OCL has been recorded in other dinosaurs, including basal ornithopods (Chinsamy et al., 1998; Horner et al., 2009), the second hypothesis appears to be the most plausible. Moreover, based on comparison of the anteroposterior width of the proximal end of the tibia, Salgado et al. (1997) proposed a lack of fully grown individuals of *G. cincosaltensis* in the fossil-bearing outcrops of the Anacleto Formation. Interestingly, even the more recent finds (Cambiaso, 2007; Cerda, 2008) consist only of small-bodied specimens. The low proportion

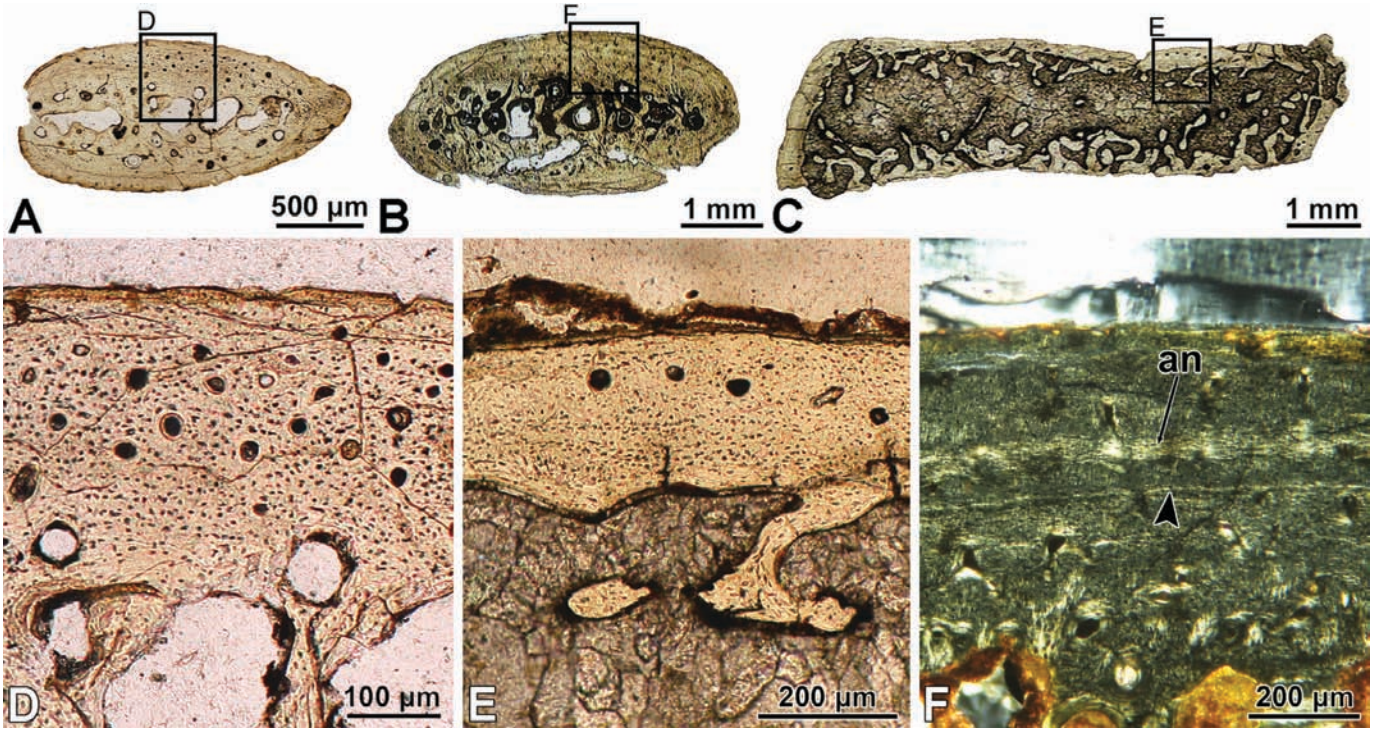

FIGURE 10. Microanatomy and histology of *Gasparinisaura cincosaltensis* dorsal ribs. **A**–**C**, general aspects of the cross-sections of different individuals (**A**, MCS-Pv 112; **B**, MCS-Pv 110; **C**, MUC-Pv 213). Note the important variation in the development of the medullary region and the cortical bone in the larger specimen (MUC-Pv 213) compared with the other samples; **D**, **E**, detail of the cortical tissue showing the prevalence of longitudinally oriented primary osteons; **F**, annulus of parallel-fibered bone in the cortical tissue. Note the presence of a birefringent line (arrowhead) below the annulus. **Abbreviation**: **an**, annulus. (Color figure available online.)

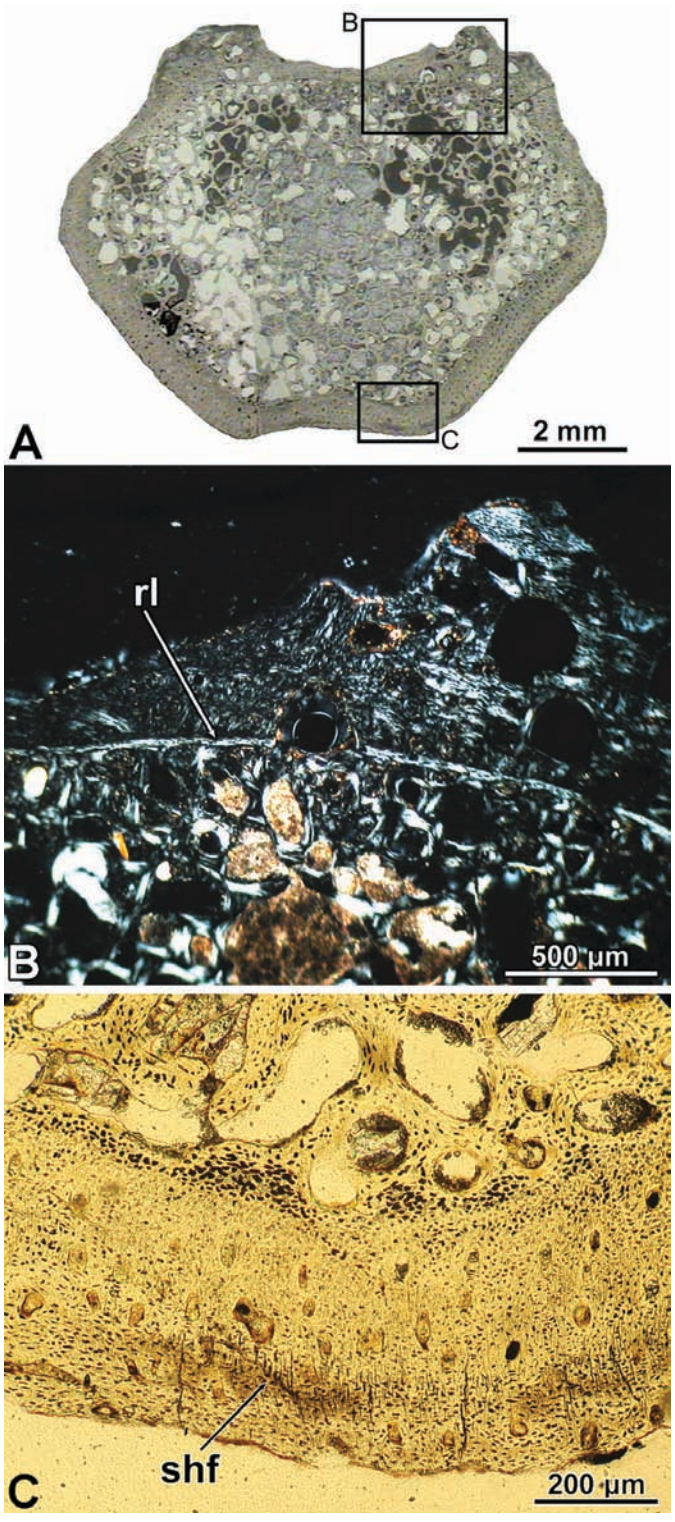

FIGURE 11. Microanatomy and histology of *Gasparinisaura cincosaltensis* caudal vertebra (MCS-Pv 109). **A**, general view of the transverse section. The element is composed of a thin cortex of compact bone surrounding a large medullary region of cancellous bone; **B**, detail of the dorsal region showing a distinct reversal line separating the endosteal and periosteal growth; **C**, close up of the ventral cortex showing abundant Sharpey's fibers. **Abbreviations**: **rl**, resorption line; **shf**, Sharpey's fibers. (Color figure available online.)

of the older ontogenetic stages in the fossil record has been proposed for the lack of an OCL in the largest individuals of other dinosaurs, including ornithopods and sauropods (Horner et al., 2009; Company, 2010).

Whether the growth strategy of *G. cincosaltensis* was actually determinate or indeterminate, it is clear that all of the specimens included in our sample (even the largest ones) were still-growing individuals, albeit at a decreased overall rate. Based on the bone microstructure, our largest specimen that we considered as 100% body size (MUC-Pv 213) is most likely only sub-adult in age. Thus, the bone microstructure suggests that sexual maturity was attained prior to skeletal maturity. The well-vascularized nature of the external cortex (which also contains vascular spaces open to the sub-periosteal surface) is indicative of active bone deposition, suggesting that even our largest individuals were actively growing at the time of death. Considering these histological findings, it appears that the adult body size of *G. cincosaltensis* was larger than registered in the known specimens (but possibly not much larger, given the evidence of slowed overall growth reflected by the presence of parallel-fibered bone and LAGs in the outer cortex of the largest specimen).

Histological Variation

Aside from the ontogenetic changes in bone microstructure, distinctive histological variation has been observed between elements of the same individual, as well as between different parts of the same element. The first important histological characteristic with variable incidence is the occurrence of annuli and LAGs, which appear to vary depending on the skeletal element, and also within the same skeletal element of the same individual. For example, in MCS-Pv 110, two LAGs and six annuli were recorded in the femur, three LAGs (without annuli) in the tibia, and one annulus in the dorsal rib. The variation in the number of growth marks in different elements of a single individual has been previously reported in other dinosaurs (Horner et al., 1999, 2000) and has also been documented in non-mammalian therapsids (Chinsamy-Turan and Ray, 2011). Hübner (2010) has also reported the variable occurrence of growth marks and the poor representation of LAGs in *Dysalotosaurus lettorwvorbecki* (between individuals, between similarly sized individuals, and within a single cross-section of a bone), which explains why they were not observed in the more limited sample of the earlier study (Chinsamy, 1995). A recent assessment of the polar hypsilophodontids also reported the histovariability in the bones, e.g., in four sections of a femur (NMV 177935) only two distal sections exhibited growth marks (Woodward et al., 2011b). It thus appears that several ornithopods seem to show a large amount of histovariability with regard to the number of the preserved growth marks. Such variations could be related to variations in the rate of periosteal deposition in different bones, varying amounts of bone drift and remodeling, as well as to local conditions of growth within a single skeletal element. Such variability further suggests that the ornithopods were highly adaptable and had variable responses in growth to local conditions. Another histological feature that appears to vary in terms of occurrence is compacted coarse cancellous bone (CCCB). In several of the more distal, proximal, or metaphyseal sections, compacted coarse cancellous bone tissue is commonly observed. In most instances, the CCCB was separated from the periosteal bone by a prominent reversal line. The occurrence of this kind of compact bone is evidence of the sequential relocation of a metaphyseal cortex into the diaphyseal cortex (Enlow, 1962).

Regarding the histological variations in the same elements of different individuals (intraspecific variation), one of the most important differences was registered in the thin sections obtained from the femora of MCS-Pv 110 and MUC-Pv 213. In both individuals a fibro-lamellar bone tissue predominated in the

inner and middle cortex, with the woven component of the fibrolamellar complex being more organized at the external cortex, and a thin layer of circumferential endosteal lamellar tissue (ICL) surrounding the medullary cavity. However, whereas the femur of MCS-Pv 110 contains annuli of parallel-fibered bone from the inner to the outer compacta, the LAGs and annuli recorded in the femur of MUC-Pv 213 are restricted to the external third of the compacta. Although the bone histology of both specimens suggests a more mature ontogenetic stage (e.g., an ICL coating the medullary cavity, well-organized intrinsic fibers at the outer cortex), MCS-Pv 110 is substantially smaller than MUC-Pv 213 (86% and 100% of LI, respectively). The development of annuli throughout the cortical bone of MCS-Pv 110 suggests that it grew more slowly than MUC-Pv 213. As mentioned above, the presence of growth marks (LAGs and annuli) indicates periodic slow down and/or complete cessation of growth. These interruptions are caused by endogenous (genetic) rhythms that become synchronized with and reinforced by environmental cycles (seasonal climatic change) (Castanet et al., 1996; Chinsamy-Turan, 2005). It is possible that the differences observed in the cortical bone of the MCS-Pv 110 and MUC-Pv 213 femora reflect varying responses to particular environmental conditions (e.g., climate and food availability/quality). Also, as proposed for other non-avian dinosaurs (Sander, 2000), the histological variation could be related to sexual dimorphism. A fast and continuous growth would be compatible with selection pressure for large size early in ontogeny (Sander, 2000). Although sample location could be considered as another source of variation, this possibility appears unlikely since except for one section from MCS-Pv 110 (MCS-Ph 114/1, which includes the distal portion of the fourth trochanter), all of the femora slices were taken from the mid-shaft (below the fourth trochanter). Because we were only able to document variation in the femora of two individuals, it would be interesting to examine a larger sample (if they became available in the future) to further understand the cause(s) of this intraspecific histovariability.

CONCLUSIONS

In all of the specimens examined, the bone cortices contain fibro-lamellar bone tissue, which qualitatively suggests rapid osteogenesis and fast growth. The presence of LAGs and/or annuli, however, indicates that this rapid growth was periodic. The growth strategy of *Gasparinisaura cincosaltensis* shows distinct changes during ontogeny: in an early phase of development (less than 60% of largest known specimen), this ornithopod experienced a fast, sustained rate of growth (possibly only altered by a slight reduction in the overall growth rate). The overall growth rate decreased later in ontogeny compared with the early phase, as shown by the change of intrinsic fiber orientation in the matrix, from a true woven-fibered matrix to a more parallel-fibered bone. As reported in other dinosaurs, *G. cincosaltensis* attained sexual maturity before attaining skeletal maturity. The growth strategy of *G. cincosaltensis* is similar to that reported in other basal ornithopods (e.g., *Orodromeus makelai*) and in general is also similar to growth dynamics reported for several other dinosaur taxa (e.g., Chinsamy-Turan 2005; Erickson, 2005). Our findings, in conjunction with recent studies (Horner et al., 2009; Hübner, 2010; Woodward et al., 2011b) suggest that ornithopods exhibited a large amount of histovariability that may be a reflection of a significant amount of plasticity in response to a range of local conditions for growth and other environmental conditions.

ACKNOWLEDGMENTS

We are most grateful to several people who allowed us to study specimens under their care: L. Salgado (Museo Universidad Nacional del Comahue) and Asociación Amigos del Museo Regional Cinco Saltos (Museo Regional Cinco Saltos). Alberto Garrido allowed us to use the Laboratory of Museo Olzacher of Zapala. Alejandra Ruffini (Centro Regional Universitario de Bariloche) is acknowledged for her technical support at the Centro Regional Universitario de Bariloche laboratory. W. Lagos and M. Gutierrez gave field assistance. We thank S. Werning and an anonymous reviewer for constructive suggestions that improved the manuscript and E. Rayfield and P. Barrett for editorial assistance. Funds from PIP 6455 and PICT 357 to L. Salgado provided financial support for different aspects of the research. The National Research Foundation, South Africa is acknowledged for funding support to A.C.

LITERATURE CITED

Botha, J., and A. Chinsamy. 2000. Growth patterns deduced from the bone histology of the cynodonts *Diademodon* and *Cynognathus*. Journal of Vertebrate Paleontology 20:705–711.

Cambiaso, A. V. 2007. Los ornitópodos e iguanodontes basales (Dinosauria, Ornithischia) del Cretácico de Argentina y Antártida. Unpublished Ph.D. dissertation, Universidad de Buenos Aires, Buenos Aires, 410 pp.

Castanet, J., H. Fracillon-Vieillont, F. J. Meurier, and A. de Ricqlès. 1996. Bone and individual aging; pp. 245–283 in B. K. Hall (ed.), Bone, Volume 7. Bone Growth. B. CRC Press, Boca Raton, Florida.

Cerda, I. A. 2008. Gastroliths in an ornithopod dinosaur from the Upper Cretaceous of Patagonia. Acta Palaeontologica Polonica 53:351–355.

Chinsamy, A. 1990. Physiological implications of the bone histology of *Syntarsus rhodesiensis* (Saurischia; Theropoda). Palaeontologia africana 27:77–82.

Chinsamy, A. 1993. Bone histology and growth trajectory of the prosauropod dinosaur *Massospondylus carinatus* Owen. Modern Geology 18:319–329.

Chinsamy, A. 1995. Ontogenetic changes in the bone histology of the Late Jurassic ornithopod *Dryosaurus lettowvorbecki*. Journal of Vertebrate Paleontology 15:96–104.

Chimsamy, A., and M. A. Raath. 1992. Preparation of fossil bone for histological examination. Palaeontologia Africana 29:39–44.

Chinsamy, A., L. Codorniú, and L. M. Chiappe. 2009. Paleobiological implications of the bone histology of *Pterodaustro guinazui*. The Anatomical Record 292:1462–1477.

Chinsamy, A., T. H. Rich, and P. Vickers-Rich. 1998. Polar dinosaur bone histology. Journal of Vertebrate Paleontology 18:385–390.

Chinsamy-Turan, A. 2005. The Microstructure of Dinosaur Bone: Deciphering Biology with Fine-Scale Techniques. Johns Hopkins University Press, Baltimore and London, 195 pp.

Chinsamy-Turan, A. 2011. Forerunners of Mammals: Radiation, Histology, Biology. Indiana University Press, Bloomington, Indiana.

Chinsamy-Turan, A., and S. Ray. 2011. Bone histology of some therocephalians and gorgonopsians and evidence of bone degradation by fungi; in A. Chinsamy-Turan (ed.), Forerunners of Mammals: Radiation, Histology, Biology. Indiana University Press, Bloomington, Indiana.

Company, J. 2010. Bone histology of the titanosaur *Lirainosaurus astibiae* (Dinosauria: Sauropoda) from the latest Cretaceous of Spain. Naturwissenschaften 98:67–78.

Constantine, A., A. Chinsamy, P. Vickers-Rich, and T. H. Rich, 1998. Periglacial enviroments and polar dinosaurs. South African Journal of Science 94:137–141.

Coria, R. A., and L. Salgado. 1996. A basal iguanodontian (Ornitischia: Ornithopoda) from the Late Cretaceous of South America. Journal of Vertebrate Paleontology 16:445–457.

Curry, K. A. 1999. Ontogenetic histology of *Apatosaurus* (Dinosauria: Sauropoda): new insights on growth rates and longevity. Journal of Vertebrate Paleontology 19:654–665.

Dingus, L., J. Clarke, G. R. Scott, C. C. Swisher III, L. M. Chiappe, and R. A. Coria. 2000. First magnetostratigraphic/faunal constraints for age of sauropod embryo-bearing rocks in the Neuquén Group (Late Cretaceous, Neuquén Province, Argentina). American Museum Novitates 3290:1–11.

Enlow, D. H. 1962. A study of the post-natal growth and remodeling of bone. American Journal of Anatomy 110:79–101.

Erickson, G. M. 2005. Assessing dinosaur growth patterns: a microscopic revolution. Trends in Ecology and Evolution 20:675–684.

Erickson, G. M., and T. A. Tumanova. 2000. Growth curve of *Psittacosaurus mongoliensis* Osborn (Ceratopsia: Psittacosauridae) inferred from long bone histology. Zoological Journal of the Linnean Society 130:551–566.

Erickson, G. M., K. Curry-Rogers, and S. A. Yerby. 2001. Dinosaurian growth patterns and avian rapid growth rates. Nature 412:429–433.

Erickson, G. M., K. Curry-Rogers, D. J. Varricchio, M. A. Norell, and X. Xu. 2007. Growth patterns in brooding dinosaurs reveals the timing of sexual maturity in non-avian dinosaurs and genesis of the avian condition. Biology Letters 3:558–561.

Fracillon-Vieillont, H., V. deBuffrénil, J. Castanet, J. Geraudie, F. J. Meurier, J. Y. Sire, L. Zylberberg, and A. de Ricqlès. 1990. Microstructure and mineralization of vertebrate skeletal tissues; pp. 471–530 in J. G. Carter (ed.), Skeletal Biomineralization: Patterns, Processes and Evolutionary Trends, Volume 1. Van Nostrand Reinhold, New York.

Hayashi, S., K. Carpenter, and D. Suzuki. 2009. Different growth patterns between the skeleton and osteoderms of *Stegosaurus* (Ornithischia: Thyreophora). Journal of Vertebrate Paleontology 29:123–131.

Horner, J. R., A. de Ricqlès, and K. Padian. 1999. Variation in skeletochronological indicators: implications for age assessment and physiology. Paleobiology 25:295–304.

Horner, J. R., A. de Ricqlès, and K. Padian. 2000. Long bone histology of the hadrosaurid dinosaur *Maiasaura peeblesorum*: growth dynamics and physiology based on an ontogenetic series of skeletal elements. Journal of Vertebrate Paleontology 20:115–129.

Horner, J. R., A. de Ricqlès, K. Padian, and R. D. Scheetz. 2009. Comparative long bone histology and growth of the 'hypsilophodontid' dinosaurs *Orodromeus makelai*, *Dryosaurus altus*, and *Tenontosaurus tilletii* (Ornithischia: Euornithopoda). Journal of Vertebrate Paleontology 29:734–747.

Hübner, T. 2010. Ontogeny in *Dysalotosaurus lettowvorbecki*. Unpublished Ph.D. dissertation, Ludwig-Maximilians-Universität München, Munich, Germany, 338 pp. Available at http://d-nb.info/1010536451/34. Accessed March 8, 2010.

Klein, N., and P. M. Sander. 2007. Bone histology and growth of the prosauropod dinosaur *Plateosaurus engelhardti* von Meyer, 1837 from the Norian bonebeds of Trossingen (Germany) and Frick (Switzerland). Special Papers in Palaeontology 77:169–206.

Klein, N., and P. M. Sander. 2008. Ontogenetic stages in the long bone histology of sauropod dinosaurs. Paleobiology 34:247–263.

Lee, A. H., and S. Werning. 2008. Sexual maturity in growing dinosaurs does not fit reptilian growth models. Proceedings of the National Academy of Sciences of the United States of America 105:582–587.

Lehman, T. M., and H. N. Woodward. 2008. Modeling growth rates for sauropod dinosaurs. Paleobiology 24:624–281.

Norman, D. B. 2004. Basal Iguanodontia; pp. 413–437 in D. B. Weishampel, P. Dodson, and H. Osmólska (eds.), The Dinosauria. Second Edition. University of California Press, Berkeley, California.

Norman, D. B., H.-D. Sues, L. M. Witmer, and R. A. Coria. 2004. Basal Ornithopoda; pp. 393–412 in D. B. Weishampel, P. Dodson, and H. Osmólska (eds.), The Dinosauria. Second Edition. University of California Press, Berkeley, California.

Novas, F. E., A. V. Cambiaso, and A. Ambrosio. 2004. A new basal iguanodontian (Dinosauria, Ornithischia) from the Late Cretaceous of Patagonia. Ameghiniana 41:75–82.

Padian, K., J. R. Horner, and A. de Ricqlès. 2004. Growth in a small dinosaurs and pterosaurs: the evolution of archosaurian growth strategies. Journal of Vertebrate Paleontology 24:555–571.

Ramos, V. A. 1981. Descripción geológica de la Hoja 33 c. Los Chihuidos Norte, Provincia del Neuquén. Servicio Geológico Nacional, Boletín 182:1–103.

Ray, S., S. Bandyopadhyay, and D. Bhawal. 2009. Growth patterns as deduced from bone microstructure of some selected neotherapsids with special emphasis on dicynodonts: phylogenetic implications. Palaeoworld 18:53–66.

Reid, R. E. H. 1996. Bone histology of the Cleveland-Lloyd dinosaurs and of dinosaurs in general. Part I: introduction to bone tissues. Brigham Young University Geology Studies 41:25–72.

Ricqlès A. de. 1980. Tissue structure of the dinosaur bone: functional significance and possible relation to dinosaur physiology; pp. 103–139 in R. D. K. Thomas and E. C. Olson (eds.), A Cold Look at the Warm-Blooded Dinosaurs. AAAS Selected Symposium 28. Westview Press, Boulder, Colorado.

Ricqlès A. de, K. Padian, and J. R. Horner. 2003. On the bone histology of some Triassic pseudosuchian archosaurs and related taxa. Annales de Paléontologie 89:67–101.

Ricqlès A. de., K. Padian, F. Knoll, and J. R. Horner. 2008. On the origin of high growth rates in archosaurs and their ancient relatives: complementary histological studies on Triassic archosauriforms and the problem of a 'phylogenetic signal' in bone histology. Annales de Paléontologie 94:57–76.

Salgado, L., R. A. Coria, and S. Heredia. 1997. New materials of *Gasparinisaura cincosaltensis* (Ornitischia: Ornithopoda) from the Upper Cretaceous of Argentina. Journal of Paleontology 71: 993–940.

Sander, P. M. 2000. Long bone histology of the Tendaguru sauropods: implications for growth and biology. Paleobiology 26:466–488.

Sander, P. M., O. Mateus, T. Laven, and N. Knötschke. 2006. Bone histology indicates insular dwarfism in a new Late Jurassic sauropod dinosaur. Nature 441:739–741.

Starck, J. M., and A. Chinsamy. 2002. Bone microstructure and developmental plasticity in birds and others dinosaurs. Journal of Morphology 245:232–246.

Stein, K., Z. Csiki, K. Curry-Rogers, D. B. Weishampel, R. Redelstorff, J. L. Carballido, and P. M. Sander. 2010. Small body size and extreme cortical bone remodeling indicate dwarfism in *Magyarosaurus dacus* (Sauropoda: Titanosauria). Proceedings of the National Academy of Sciences of the United States of America 107:9258–9263.

Varricchio, D. J. 1993. Bone microstructure of the Upper Cretaceous theropod dinosaur *Troodon formosus*. Journal of Vertebrate Paleontology 13:99–104.

Varricchio, D. J. 1997. Growth and embryology; pp. 282–288 in P. J. Currie and K. Padian (eds.), Encyclopedia of Dinosaurs. Academic Press, San Diego.

Winkler, D. 1994. Aspects of growth in the Early Cretaceous Proctor Lake ornithopod. Journal of Vertebrate Paleontology 14(3, Supplement):53A.

Woodward, H. N., J. R. Horner, and J. O. Farlow. 2011a. Osteohistological evidence for determinate growth in the American alligator. Journal of Herpetology 45:339–342.

Woodward, H. N., T. H. Rich, A. Chinsamy, and P. Vickers-Rich. 2011b. Growth dynamics of Australia's Polar dinosaurs. PLoS ONE 6:e23339. doi: 10.1371/journal.pone.002339

Submitted May 22, 2011; revisions received October 28, 2011; accepted November 20, 2011.

Handling editor: Emily Rayfield.